Two-particle transfer and pairing correlations: interplay of reaction mechanism and structure properties

Andrea VITTURI[1] and Hugo M. SOFIA[2]

[1] *Dipartimento di Fisica e Astronomia "G.Galilei" and INFN, Padova, Italy*
[2] *CNEA, Departamento Fisica Teorica, Tandar, Buenos Aires, Argentina*

Two-particle transfer processes induced by light and heavy ions are known to be an ideal dynamical tool for extracting information on nuclear pairing correlations. The procedure is however not unique and different reaction mechanism models (ranging from microscopic correlated successive one-particle transfer to collective macroscopic models) can be introduced to establish a link with the structural aspects of initial and final states. We breafly review the subject with special attention to the novel features arising in systems close to the drip lines from the weak binding situation and the consequent role of continuum states.

Subject Index: 212,221,227

§1. Pairing and spatial correlations

Two-particle transfer processes induced by light ions (reactions as (t,p), (p,t), (^{3}He,n), (α,d)) or heavy ions are considered the ideal tool to study the dynamical aspects of pairing correlations, since all these reactions do explore precisely the full radial properties of pair correlations.[1)–3)] The situation is however different, for example, from low-energy one-step Coulomb excitation, where the excitation probability is directly proportional to the B(Eλ) values. Here the reaction mechanism is much more complicated and not well established, so that the possibility of extracting spectroscopic information on the pairing field is not straightforward.

It is often assumed that the cross section for two-particle transfer will scale with the square of the matrix element of the pair creation (or removal) operator $T_0^+ = \sum_j [a_j^+ a_j^+]_{00}$ (or $T_0^- = \sum_j [a_j a_j]_{00}$. All along this survey, we will restrict ourselves to the effect of the pairing interaction between identical particles (T=1) acting on the 0^+ channel. These matrix elements will be enhanced in presence of strong pairing correlations, due to the collective features of initial and final states. In this perspective in order to define a quantitative measure of the collectivity of pairing modes one could compare with single-particle pair matrix elements to define "pairing single-particle units" and therefore pairing enhancement factors. As a first example of these enhancements, we show in figure 1 the prediction for the pair addition response in the pair vibrational scheme around a closed shell (^{208}Pb). This amounts to the squared pair creation matrix elements connecting the ground state of ^{208}Pb with all 0^+ states in ^{210}Pb, as a function of the excitation energy in ^{210}Pb. Pairing correlations are here treated in RPA or TDA, and the corresponding responses are compared with the unperturbed values at the HF level. The figure clearly shows the strong pairing collectivity of the ground state (PV, Pairing Vibration), as well as the appearence of a collective state at high excitation energy (GPV, Giant Pairing

Vibration). As a second example in an open shell case (so called pairing rotational regime) we show in figure 2 the pair addition strength function obtained by Khan etal[4] within the continuum HFB+QRPA in the very neutron-rich ^{22}O, again compared to the unperturbed one. It is clearly visible the effect of the residual pairing interaction in moving to lower energies the pair strength and in enhancing its value.

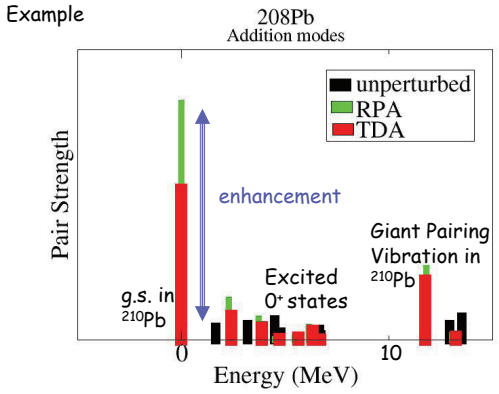

Fig. 1. Pair addition response to 0^+ states in ^{210}Pb, as a function of the excitation energy in ^{210}Pb. The results of the (discrete) correlated RPA and TD models are compared with the unperturbed single-particle HF ones.

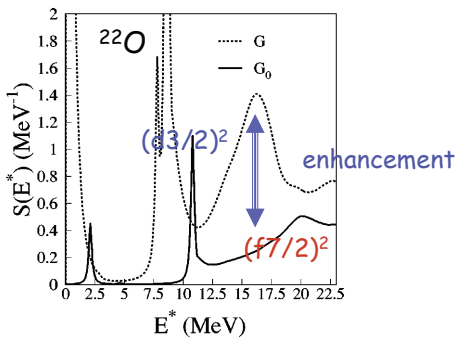

Fig. 2. the pair addition strength function obtained by Khan etal[4] within the continuum HFB+QRPA in the very neutron-rich ^{22}O, compared to the unperturbed one.

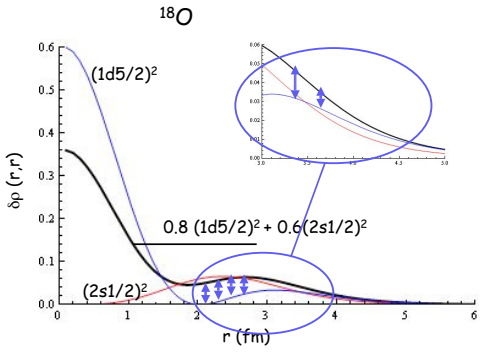

Fig. 3. Local pair addition transition density in ^{16}O (leading to ^{18}O). The cases of pure $(1d5/2)^2$ and $(2s1/2)^2$ are compared with the case of correlated wave function.

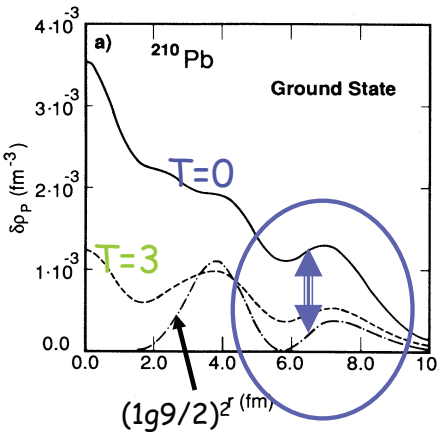

Fig. 4. Local pair addition transition density in ^{208}Pb (leading to ^{210}Pb). The case of pure $(2g9/2)^2$ is compared with the case of correlated QRPA wave function (at different temperatures

But the two-particle transfer process in not sensitive to just the pair matrix

element. We have to look at the radial dependence of the pair transition density, which is relevant for the reaction mechanism associated with pair transfer processes. As examples we show in Figs. 3 and 4 the comparison with pure single-particle configurations in the case of the addition mode around ^{16}O (i.e. the ground state of ^{18}O) and ^{208}Pb (i.e. the ground state of ^{210}Pb).[5] The comparison is done directly on the local transition density ($\delta\rho_P(r,r)$). The enhancement effect of the correlation is rather clear, in particular in the strongly correlated ground state of ^{210}Pb. In Fig. 4 we also display the case at finite temperature (T=3 MeV) to show how a large value of the temperature (beyond the critical value) can practically wash out the pairing correlations.

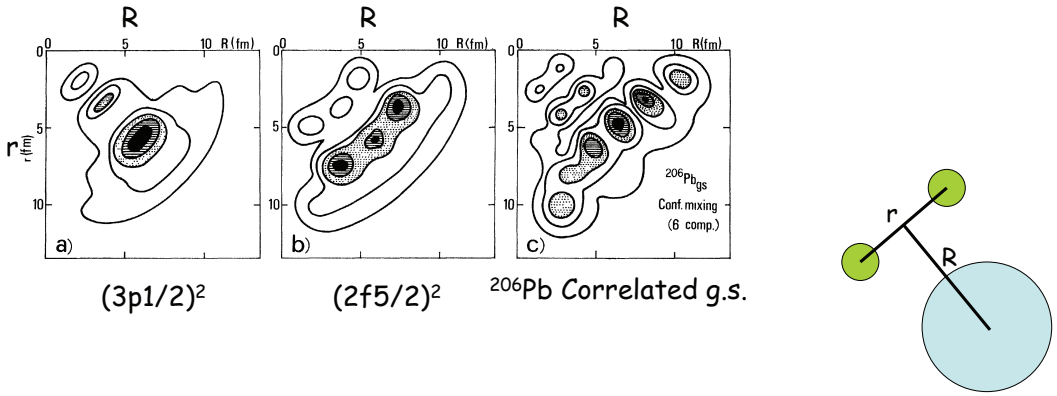

Fig. 5. Square of the pair removal transition density in ^{208}Pb (leading to the ground state of ^{206}Pb). The correlated RPA wave function is compared with the cases of pure $(3p1/2)^2$ and $(2f5/2)^2$. The transition density is shown as a function of $\vec{R} = (\vec{r_1} + \vec{r_2})/2$ and $\vec{r} = \vec{r_1} - \vec{r_2}$. From ref.[6]

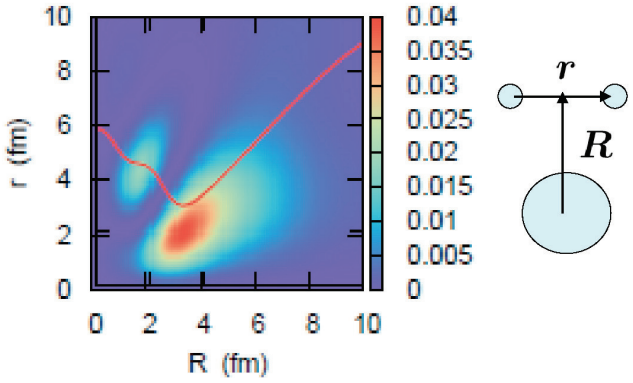

Fig. 6. Two-particle probability describing the two valence neutrons in ^{11}Li. From ref.[7]

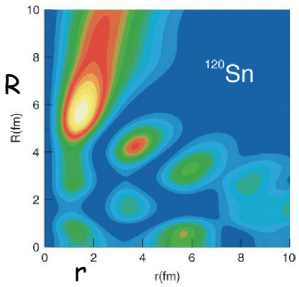

Fig. 7. Square of the pair transition density in ^{120}Sn, described within the HFB formalism. From ref.[8]

The spatial correlations induced by the pairing interaction are further evidenced

by the non-local pair transition density $\delta\rho_P(r_1, r_2)$. This is shown in figures 5,6 and 7 as contour plots as a function of center-of-mass coordinate $\vec{R} = (\vec{r_1} + \vec{r_2})/2$ and relative coordinate $\vec{r} = \vec{r_1} - \vec{r_2}$. As shown, for example, in figure 5, which refers to the description of the removal pairing mode corresponding to the gs of ^{206}Pb, in the case of pure two-particle configurations the pair transition density displays a symmetric behaviour with respect to R and r, while the correlated RPA case favours the "clustering" of the two neutrons, reducing the relative distance. On the other side the "pair" moves outside, so enphatizing the "surface" character of the pairing correlations. Similar features can be seen in figure 6, which describes the correlated pair of valence neutrons in ^{11}Li, and in figure 7, which refers to the superfluid HFB pairing density in ^{120}Sn.

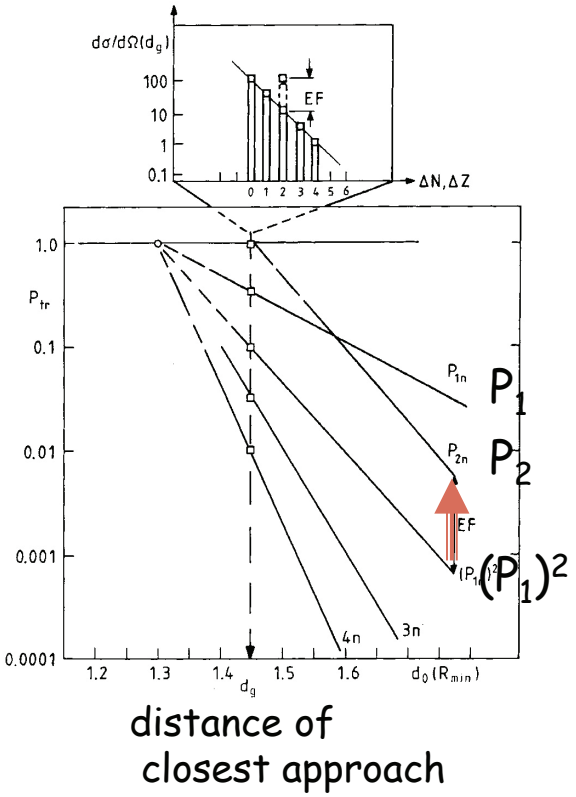

Fig. 8. Schematic picture illustrating the method for extracting the "pair enhancement factor" from one- and two-particle transfer probabilities plotted as a function of the classical distance of closest approach

§2. Two-particle transfer probabilities: experimental issues

We have so far discussed "theoretical" pairing enhancement factors. The situation is more complex from an experimental point of view, for the difficulty in defining

the "single-particle" reference values. A popular method used in heavy-ion reactions is based on the comparison of one- and two-particle transfer cross sections.[2)] Using semiclassical arguments for the description of the relative motion one plots transfer probabilities not as function of the scattering angle, but as function of the distance of closest approach of the corresponding classical trajectory (cf. figure 8). Due to the exponential behaviour of the particle-transfer formfactors the probabilities also display an exponential behaviour. In the hypothesis of a sequence of successive transfer of two complitely uncorrelated particles, by squaring the "experimental" probability P_1 for one-particle transfer one obatains the "expected" probability $P_2 = (P_1)^2$ for two-particle transfer, with a slope parameter double then the one for one-particle transfer . The comparison with the "experimental" P_2 probability gives the "pair enhancement" factor, measuring therefore the increase (due to the pairing correlations) in two-particle transfer cross sections with respect to the expected uncorrelated case. Two examples of the method are given in figures 9 and 10, for neutron and proton pair transfer respectively. The magnitude of the arrows indicates the "enhancement factors" (EF).

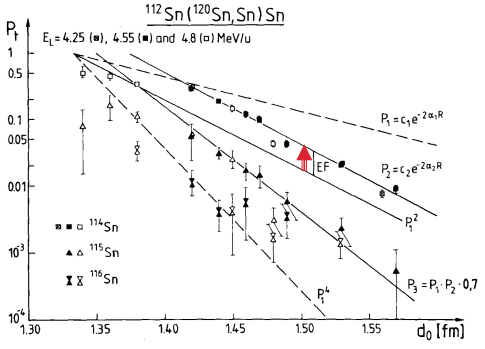

Fig. 9. One-, two- and multi-neutron transfer probabilities plotted as a function of the classical distance of closest approach for the reaction ^{112}Sn(^{120}Sn,Sn)Sn. From ref.[2)]

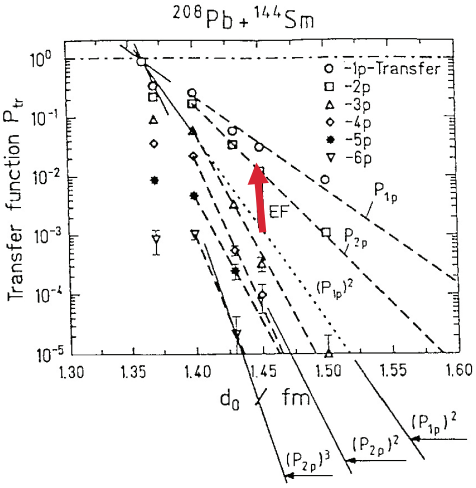

Fig. 10. One-, two- and multi-proton transfer probabilities plotted as a function of the classical distance of closest approach for the reaction ^{208}Pb + ^{144}Sm. From ref.[2)]

A severe problem from the experimental point of view is the selection of the final states and their angular momenta. For even-even nuclei, for example, we expect that the 0^+ states will be those displaying the features associated with the pairing degree of freedom, and among the 0^+ state it is the ground state (or eventually the high-lying giant pairing vibrational state GPV) to show collective features and enhanced transitions. Good energy resolution and good angular distributions are therefore essential to select the different states. This is easier in the case of two-particle transfer processes induced by light ions, as e.g. (p,t) or $(^3He, n)$, since in this case the angular distributions show clear shapes associated with the value of transfer

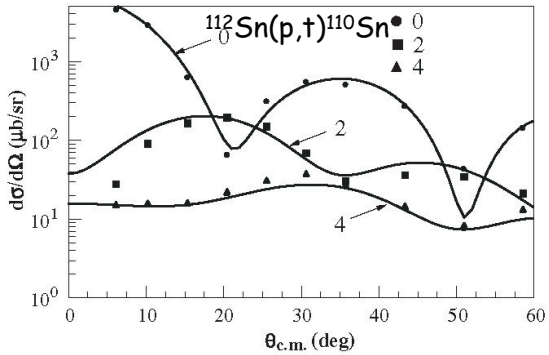

Fig. 11. Angular distributions for two-neutron transfer reaction populating states in ^{110}Sn with different angular momenta. From ref.[9)]

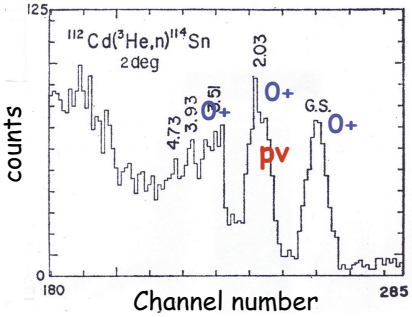

Fig. 12. Excitation function at forward angle for two-proton transfer reaction populating ^{114}Sn. From ref.[10)]

angular momentum and in particular a strong forward peak for $L = 0$ transfer (cf. figure 11). A beautiful example of forward-angle selectivity is displayed in figure 12 for a proton-pair transfer reaction, showing clearly the peaks associated with the ground state (gs) and the 2p-2h proton pairing vibration (pv) in ^{114}Sn associated with the Z=50 closed shell. The importance of a good energy and angular resolution is exemplified in figure 13, where one displays the predicted total excitation function for two-neutron pick-up in the reaction ^{120}Sn(p,t)^{118}Sn(λ). The final states are described in RPA and the contributions of the different multipolarities are given separately. The figure shows clearly that the 0^+ states are embedded in a large background of other multipolarities. This may be one of the reason for the so-far unsuccessfull search for the Giant Pairing Vibration.

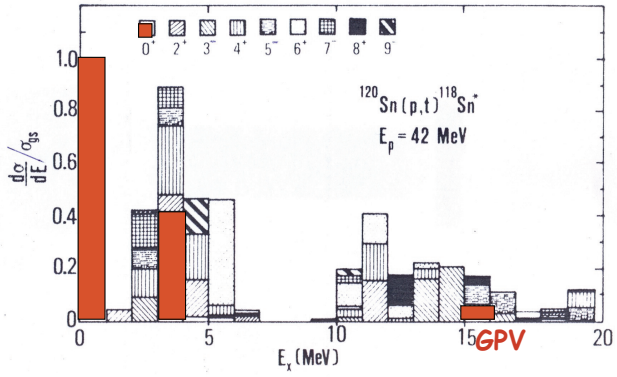

Fig. 13. Predicted excitation function for two-neutron pick-up in the reaction ^{120}Sn(p,t)^{118}Sn(λ). The contributions of the different multipolarities are given separately. From ref.[?]

The angular momentum selection is even more complex in the case of heavy-ion induced reactions, since in this case all angular distributions to all final states are peaked at the grazing angle, irrespectively of the angular momentum transfer. A

typical example is given in figure 14.

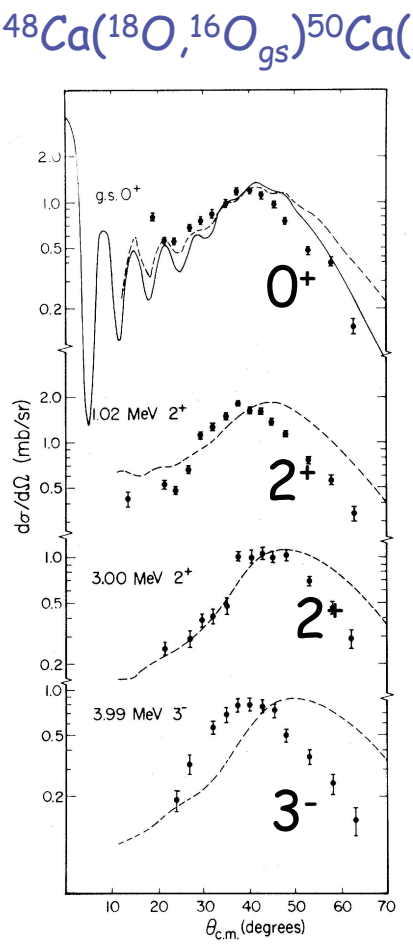

Fig. 14. Angular distributions leading to different final states with different multupolarity λ in ^{50}Ca in the reaction ^{48}Ca,^{18}O,$^{16}O_{gs}$)^{50}Ca(λ). From ref.[12)]

A further problem arises from the kinematical "Q-value" effects. These include all effects arising from the dynamics and matching of the scattering orbits, from one side, and from the change of the internal bound states in the process of transfer between the two nuclei. The result is the occurrence of a favoured "Q-value window" centered around an optimal Q-value Q_{opt}, the final cross section being modulated by a Q-value factor F(Q) which can be approximated as $F(Q)$=exp(-$k(Q-Q_{opt})^2$). The Q_{opt} and the parameter k depend on the masses m_a and m_A and charges z_a and z_A of colliding nuclei, mass m and charge z of the transferred particle, bombarging energy E and angular momentum transfer. In the particular case of $L = 0$ transfer the Q_{opt} acquires the form $Q_{opt} \approx (z/z_A - z/z_a)E_c + (m/m_A - m/m_a)(E - E_c)$, E_c being the value of the Coulomb barrier . The net effect of the Q-value factor is that, according to the masses involved, strong collective pairing states (as e.g. the

ground state) may be in some case completely quenched with respect to weaker (but Q-value favoured) excited state. An illustrative example is given in figure 15, where the experimental cross sections for two-neutron transfer in the reaction ^{96}Zr+ ^{40}Ca leading to ^{42}Ca mass partition is shown as a function of total kinetic energy loss (or equivalently in excitation energy). In this case the Q_{opt} is approximately zero, and the ground state (having a rather positive Q-value) falls outside the optimum Q-value window. On the other side, the maximum probability will be centered on large excitation energy, in spite of the expected weaker pairing strength.

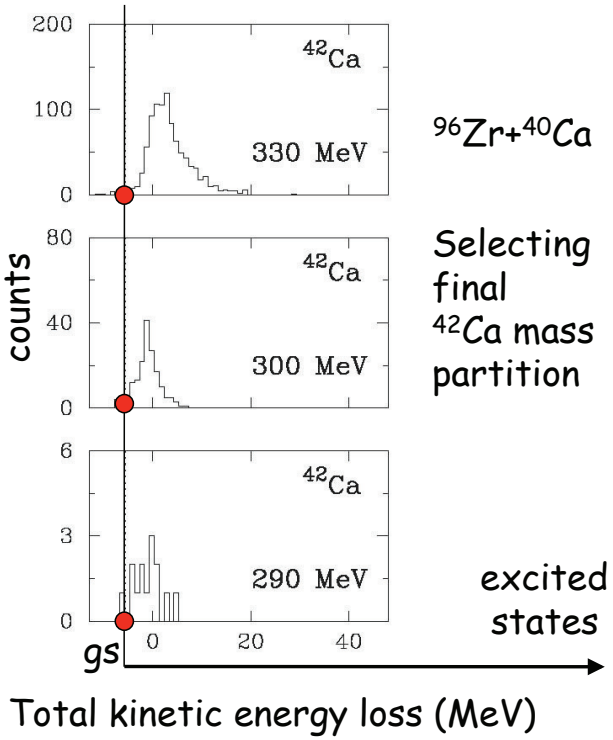

Fig. 15. Experimental cross sections (in counts) for two-neutron transfer in the reaction ^{96}Zr+ ^{40}Ca leading to ^{42}Ca mass partition as a function of total kinetic energy loss (or equivalently in excitation energy). Different bombarding energies around the Coulomb barrier are considered. From ref.[13)]

According to the specific reaction used, therefore, one gets a different position of the ground state in the Q-value window. As an example we plot in figure 16 the Q-value factor for a two-neutron stripping reaction leading to ^{210}Pb induced by different projectiles (^{96}Zr, ^{18}O and ^{6}He). It is clear that *ceteris paribus* the ground state transition is favoured by the Q-value in the first two cases, while transitions to high-lying states are strongly enhanced in the last case. The width of Q-value gaussian depends on the bombarding energy, and figure 17 shows the corresponding Q-value functions for the same reaction but different energies. Similar to the case of other reactions, as for example Coulomb excitation, lower bombarding energies give rise to narrower Q-value windows.

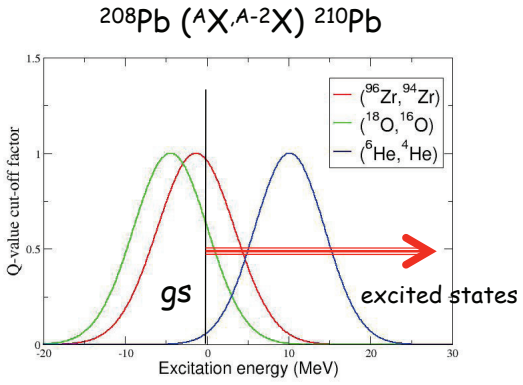

Fig. 16. Q-value factor as a function of the energy of the final state in ^{210}Pb for different reactions, at a bombarding energy of 1.2 E_B (E_B being the energy of the Coulomb barrier).

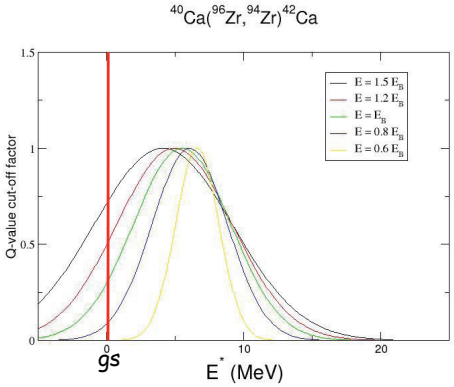

Fig. 17. Q-value factor as a function of the energy of the final state in ^{42}Ca for the reaction ^{40}Ca(^{96}Zr,^{94}Zr)^{42}Ca, at different values of the bombarding energy.

To better illustrate how the intrinsic pairing strength distribution is modulated by the Q-value factor we compare in figures 18 and 19 the pair addition strenght in ^{210}Pb , already shown in figure 1, with the corresponding cross sections for two-neutron transfer reactions leading to the same final states. In figure 18 the reaction is ^{208}Pb(^{18}O,^{16}O)^{210}Pb, in figure 19 the considered reaction is ^{208}Pb(^{6}He,^{4}He)^{210}Pb. In both cases the pairing strength functions obtained in RPA and TD are compared with the unperturbed ones. It is clear that the Q-value factor modulates the final cross sections differently in the two cases, favouring the transition to the ground state in the former case and the transition to the GPV in the latter case.

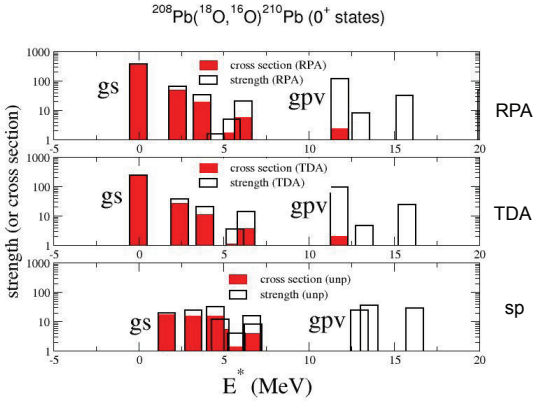

Fig. 18. Pair addition response to 0^+ states in ^{210}Pb, as a function of the excitation energy in ^{210}Pb, compared with the estimated cross sections for the reaction ^{208}Pb(^{18}O,^{16}O)^{210}Pb. Both strength and cross sections are normalized to the grouns-state values.

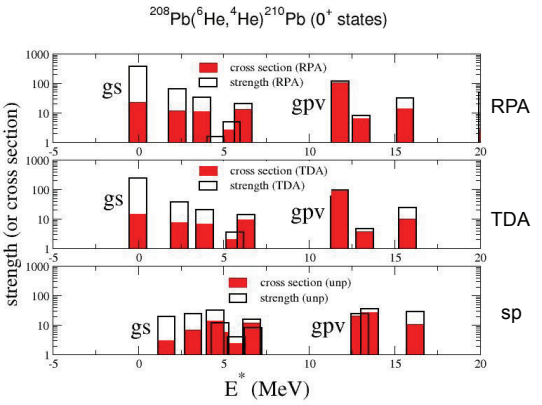

Fig. 19. Pair addition response to 0^+ states in ^{210}Pb, as a function of the excitation energy in ^{210}Pb, compared with the estimated cross sections for the reaction ^{208}Pb(^{6}He,^{4}He)^{210}Pb. Both strength and cross sections are normalized to the grouns-state values.

§3. Models for two-particle transfer reactions

One can see from the simple examples shown in Sect. 1 that the effect of the pairing on the spatial properties of the pair densities is clearly established. The difficult point is to clarify how the structure properties enter into the reaction mechanism. To this end one needs reliable models for the description of the reaction mechanism. There are at present in the literature a large number of different approaches, all trying to reduce the actual complexity of the problem, which is a genuine four-body scattering (the two cores plus the two transferred particles). Note also that different approaches are used in the case of in the case of light ions (as (p,t) reactions, not discussed here) and heavy-ion induced reactions (where one may need detailed information on the wave functions in both target and projectile, but on the same time the reaction is mainly surface-peaked and semiclassical descriptions may apply).

Motivated by the complexity of the traditional microscopic description of two-particle transfer processes, an alternative macroscopic framework has been suggested, the inspiration for its implementation being drawn from the treatment of inelastic excitations to collective surface modes. The simplicity and the intuitive appeal of the macroscopic model for inelastic excitation have, in fact, made this approach the favourite tool in the spectroscopy of low-lying vibrational states. In order to realize the analogy with the case of inelastic excitations, it may be useful just to summarize the main points in this case. Also in the case of excitation one can start from a microscopic approach where the radial matrix elements are given in the form

$$F(R) = \int dr \delta\rho(r) V(R-r)$$

namely as the folding of the external one-body field $V(R-r)$ (generated by the projectile in the case of target excitation) with the transition density $\delta\rho(r)$ for the inelastic process, described for collective states in terms of the superposition of particle-hole excitations. The fundamental idea of the macroscopic model for inelastic excitations is to interpret the superposition of particle-hole excitations as representing a state of collective nuclear motion in which the density of the system deviates from its (spherical) equilibrium shape. The deformed surface is parametrized in terms of the variables $\alpha_{\lambda,\mu}$ which measure the extent of the deviation for the different multipolarities. To leading order the forces which tend to restore the spherical shape of the system are directly proportional to these elongation variables. This ensures the harmonic character of the motion and also provides a reason why these elementary modes of nuclear motion are known as surface vibrations (for the present qualitative discussion we may drop for simplicity the indices λ, μ in α). Establishing a connection between the changes in the radius and the vibrations of the density at the nuclear surface, one has

$$\delta\rho = (\partial\rho/\partial\alpha)\alpha = (\partial\rho/\partial r) R\alpha$$

and therefore the way is open to introduce a transition density of the form

$$\delta\rho = \beta_\lambda R(d\delta/dr)$$

and, by folding, the subsequent familiar form for the radial part of the form factor

$$F(r) = \beta_\lambda R dU/dr$$

in terms of the ionion potential, U, is obtained. The amount of collectivity is governed by the deformation parameter , namely the matrix element of the surface deformation operator between the ground state and the excited state, a number which can be directly related to experimentally accessible quantities like, for instance, the B[E(λ)] values provided by a Coulomb excitation experiment.

The generalization of these concepts to the case of two-particle transfer processes[14] requires a number of crucial (and not trivially acceptable) steps. The first is the interpretation of the local generalized particle-particle transition density $\delta\rho_P^+$ (and $\delta\rho_P^-$+ P (and $\delta\rho_P^-$) associated with the pair addition (and removal) process as an operator of one-body character. The formal use of this generalized density is contemplated in connection with an external field which is a function of just one coordinate and therefore in analogy to the ordinary one-body operator. The form factor for the excitation of a pair-addition mode therefore takes the form

$$F^+(R) = \int dr \delta\rho_P^+(r) V(R-r)$$

i.e. the folding of the pair transition density for the corresponding collective mode with the external field experienced by the nucleons in the target. The pair-addition transition density can be microscopically expressed, in the case of the collective pairing mode, as a proper coherent superposition of particle-particle configurations. The subsequent step toward the macroscopic model is the choice of a proper macroscopic variable to describe the collective motion in the pairing degree of freedom. Pair vibrations (rotations) are associated with modes which relax the conservation of the number of particles and combine states corresponding to different isotopes (or isotones). In this respect the natural variable for these modes is the deviation ΔA in mass from the initial partition. In order to construct the macroscopic transition density we also assume here that the changes in the potential acting between the two ions arise from the modification in the density as a function of particle number. Thus

$$\delta\rho_P = (\partial\rho/\partial\Delta A)\Delta A = (R/3A)\ (\partial\rho/\partial r)\Delta A.$$

In this expression we have made use of the saturation of the equilibrium density in nuclei of mediumlarge size and therefore have established a direct link between an eventual increase in the number of particles in the system with the change of density at the nuclear surface that is necessary in order to accommodate them. From this argument we can infer a model function for the pair transition density, this time in the form

$$\delta\rho_P = \beta_P (r/3A) d\rho/dr.$$

The pairing deformation parameter β_P plays a role entirely analogous to the surface deformation parameter β_λ. It scales the radial shape of the pair transition density and therefore is the quantity that measures the strength represented in the mode. More collective or less collective modes are no longer distinguished by different radial

functional dependences in the transition densities, but rather by their overall size specified by β_P. The pay-off of this simple parametrization of the pair transition density is collected when we construct the matrix elements of the field that generates the excitation of the modes. The transition densities for surface and pairing modes become proportional to each other, and it is possible in the treatment of pair transfer to adopt techniques originally developed for the study of inelastic processes. In fact, by a folding procedure one gets for the pair-transfer form factor the expression

$$F^+(r) = (\beta_P/3A)RdU/dr,$$

namely an expression formally equal to the one for inelastic excitation. Indeed, exploiting the correspondence $\beta_\lambda = \beta_P/3A$ one can directly take over existing computer codes, designed for the calculation of angular distributions of the excitation of inelastic surface modes. It must be emphasized that the previous expression represents only a formal equivalence, insofar as there is no fundamental connection between the deformation parameters for collective surface and pairing modes. Thus this correspondence is only meant as an operational prescription to relate the role played by both quantities in the reaction formalism.

These approach to two-particle transfer reactions has been widely used in the literature both in the full macroscopic limit and in its semi-microscopic version. We recall once more that in a semi-microscopic approach the reaction mechanism is described as a one-step di-neutron (cluster) transfer and the microscopy amounts to construct a formfactor obtained by double-folding the full microscopic pair transition densities of initial and final states with some nucleon-nucleon interaction or by simple folding of microscopic pair density in the target with the one-body mean field of the projectile. In the complete macroscopic approach all microscopy is simply hidden (or better embedded) in the value of the β_P parameter, obtained by integrating the microscopic $\delta\rho_P(r)$.

All such approaches only involve (at different levels) the local transition densities and do not exploit the full non-local features of the pair correlation. A fully microscopic approach is instead the one in which the traditional formalism for the description of one-particle transfer processes in heavy-ion reactions is extended to two-particle transfer.[1),2),15),16)] It may be useful to remind the reader that the process in which a nucleon is transferred is already a rather complicated one, since it amounts to a rearrangement in the state of motion of all the nucleons which are present in both projectile and target. A series of basic assumptions are normally used to reduce the complexity of such a problem. The assumption of inert cores simplifies the problem into a transition involving a single nucleon, generated by the action of a one-body operator. Such an effective one-body field is normally taken as the mean field that binds the nucleon either in the entrance channel (prior representation) or in the exit channel (post representation), and the transition amplitude is related to radial matrix elements (form factors) involving the folding of initial and final one-particle wavefunctions (centred at projectile and target positions, respectively) with either one-body potential. Since in this approach the interaction responsible for the transfer is attributed to the one-body field generated by the target (or projectile) the only way in which such an interaction can produce a rearrangement of two nucleons

in a two-particle transfer process is by a two-step process in which the particles are transferred successively, since it is inherent to the concept of the one-body operator that it can act only on one particle at a time. In addition, the collective nature of initial and final states of the pair bound states introduces a decomposition of the transfer amplitudes into coupled single-particle configurations, a complexity to which one has to add the large range of possible intermediate states in the odd systems, i.e. the intermediate steps leading to the final mass partition.

Within this approach based on sequential two-step process the pairing enhancement comes from the coherent interference of the different paths through the different intermediate states in (a-1) and (A+1) nuclei, due to the correlations in initial and final wave functions. Basis ingredients of the calculation are the individual formfactors for one-particle transfer and the microscopic pairing correlated wave functions. Since such fully quantal calculations are rather complex (taking into account full recoil), semiclassical approximation scheme are commonly used (although with approximate treatment of recoil), by double integrating in time the two successive formfactors along the classical trajectory for the relativa motion.

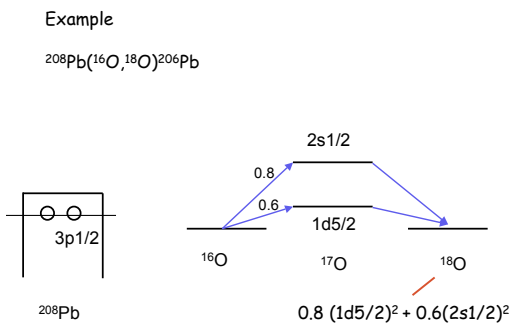

Fig. 20. Scheme of two-particle transfer etc in ^{18}O.

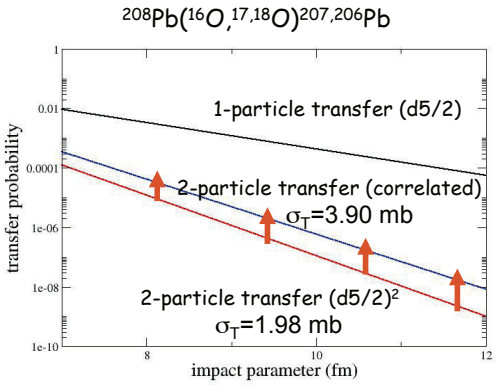

Fig. 21. Probabilities for one-, two- (uncorrelated) and two-particle (correlated) transfer as a function of the impact parameter

As an example, we consider the pair transfer reaction ^{208}Pb(^{16}O, ^{18}O$_{gs}$)^{206}Pb$_{gs}$ at a bombarding energy around the Coulomb barrier. We assume that the two particles are trasferred from the 3p1/2 level in ^{208}Pb into a correlated ground state of ^{18}O, taken as a linear combination of $(1d5/2)^2$ and $(2s1/2)^2$ (cf. Fig. 20). The effect of the correlation on the two-particle transfer probability is evident from Fig. 21, where the probabilities for one and two-particle transfer are shown as a function of the impact parameter. The results for the correlated case is compared with the corresponding values for the uncorrelated one in which the two particles are simply trasferred in pure $(1d5/2)^2$ orbits. Integrating over the impact parameter one obtains a two-particle transfer cross section which is approximately a factor two enhanced with respect to the uncorrelated case (3.90 mb with respect to 1.98 mb in the case of pure $(1d5/2)^2$ case).

As we move closer or even beyond the drip lines the previous picture is inevitably

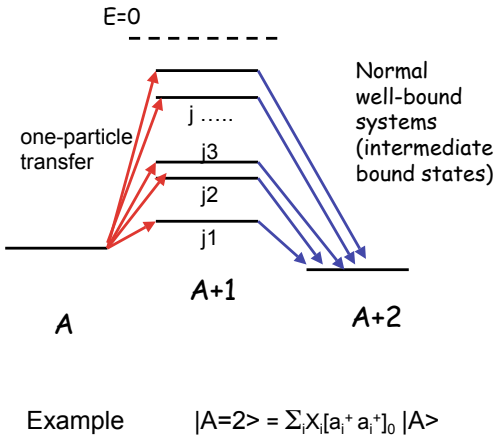

Fig. 22. Scheme of two-particle transfer for normal systems

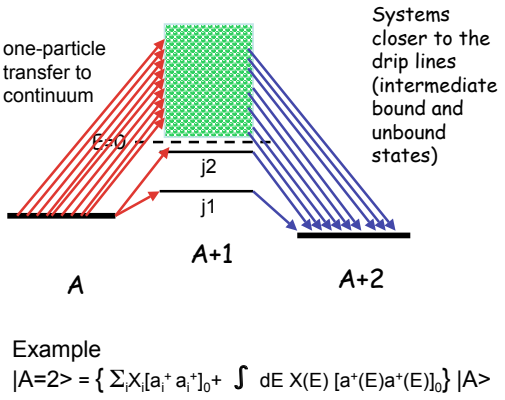

Fig. 23. Scheme of two-particle transfer for systems towards the drip line

modified. As schematically shown in Figs. 22-23, we move from a situation in which all relevant intermediate states are bound (Fig. 22), to situations in which only part of these states are bound (Fig. 23), finally even reaching at the drip line situations in which no bound intermediate states are present and only due to the pairing interaction the (A+2) system becomes bound. Typical examples are given by the so-called Borromean nuclei such as ^{11}Li or ^{6}Li whose ground states are bound in spite of no available bound states in ^{10}Li or ^{5}He. For weakly-bound systems at the drip lines it is therefore mandatory to include in the models the positive energy part of the spectrum. This opens a full new scenario where new models and approaches are acting. If one wants to still use the same formal machinary used with bound states, one has to resort to the some form of discretization of the continuum and in this framework the recipe of the so-called CCDC model is most popular and successful. We should note, however, that coupled channel descriptions based on discretization of the continuum can be accurate when a proper choice is made of the number of discrete states, of the energy mesh and of the energy cutoff. This may imply, even in simplified cases, the use of a rather large (and unpracticable) number of channels. The use of a more restricted number of channels may lead to misleading results. In this line simple models (for example one-dimentional) that may be solved "exactly" may be useful in testing the different assumptions and the range of validity of the different formalisms (cf. e.g. refs.[17)–19)]). In the case of two-particle transfer processes the intrinsic complexity of the reaction increases the uncertainties connected with the description of the continuum, and it is not surprising if the problem is still under debate and a satisfactory solution is still missing.

References

1) Broglia RA and Winther A 1991 *Heavy-Ion Reactions: Lecture Notes*, Addison-Wesley, New York
2) von Oertzen W and Vitturi A 2001 *Rep. Prog. Phys.* **64** 1247
3) Corradi L, Pollarolo G and Szilner S 2009 *J. Phys. G: Nucl. Part. Phys* **36** 113101

4) Khan E, Sandulescu N, Nguyen Van Giai, and Grasso M 2004 *Phys. Rev. C* **69** 014314
5) Lotti P, Cazzola F, Bortignon P F, Broglia R A, and Vitturi A 1989 *Phys. Rev.* C **40** 1791
6) Catara F, Insolia A, Maglione E, and Vitturi A 1984 *Phys. Rev.* C**29** 1091
7) Hagino K, Sagawa H, Carbonell J, and Schuck P 2007 *Phys. Rev. Lett.* **99** 022506
8) Pillet N, Sandulescu N, and Schuck P, 2007 *Phys. Rev.* C**76** 024310
9) P. Guazzoni *etal* 2006 *Phys. Rev. C* **74** 054605
10) Fielding HW *et al* 1977 *Nucl. Phys. A* **281** 389
11) Bortignon PF *etal* 1986 *Phys. Scr.* **34** 678
12) Petersen JF *etal* 1976 *Phys. Rev. Lett.* **36** 307
13) Corradi L *etal* 2011 *Phys. Rev. C* **84** 034603
14) Dasso CH and Pollarolo 1985 *Phys. Lett. B* **155** 223; Dasso CH and Vitturi A 1986 *Phys. Lett. B* **179** 337; Dasso CH and Vitturi A 1987 *Phys. Rev. Lett.* **59** 634
15) Bayman BF and Chen J 1982 *Phys. Rev. C* **26** 1509; Maglione E, Pollarolo G, Vitturi A, Broglia RA and Winther A 1985 *Phys. Lett. B* **162** 59
16) Potel G, Barranco F, Vigezzi E etal 2010 *Phys. Rev. Lett.* **105** 172502; Potel G, Marini F, Idini A, Barranco F, Vigezzi E, Broglia RA, http://arxiv.org/abs/1105.6250
17) Dasso CH and Vitturi A 2009 *Phys. Rev. C* **79** 064620
18) Pérez-Bernal F and Vitturi A 2009 *AIP Conf. Proc.* **1165** 305
19) Vitturi A and Pérez-Bernal F 2010 *Nucl. Phys.* **A834** 428c